Highly rechargeable $Li_xMnO_{2+\delta}$ oxides synthesized via low temperatures techniques

S. Franger[a], S. Bach[a,*], J.P. Pereira-Ramos[a], N. Baffier[b]

[a]*CNRS, UMR 7582, LECSO, 2 rue Henri Dunant, 94320 Thiais, France*
[b]*CNRS, UMR 7574, LCAES, 11 rue Pierre et Marie Curie, 75005 Paris, France*

Abstract

The synthesis of lithiated manganese oxides $Li_xMnO_{2+\delta}$ obtained via a sol–gel process combined with an ion-exchange reaction is reported. The electrochemical performances are strongly dependent on the heat-treatment of the Li-exchanged compound obtained after the ion-exchange procedure. The best results are obtained for the sample heat-treated at 300°C and which corresponds to a mixture of a spinel phase ($a = 8.16$ Å) and a lamellar phase. Galvanostatic cycling tests in the potential window 4.2/2 V show that a stable capacity of 155 mAh/g is achieved after 20 cycles performed at C/20 rate. © 2001 Elsevier Science B.V. All rights reserved.

Keywords: Lithium batteries; Galvanostatic cycling test; Sol–gel process

1. Introduction

Secondary lithium batteries have been studied for the past two decades, because they exhibit the highest specific energy among the rechargeable batteries. From the point of view of starting material in these batteries, price and toxicity of the system lithium–manganese-oxide as the spinel $LiMn_2O_4$ has a considerable advantage over $LiNiO_2$ and $LiCoO_2$, for its use as cathodic material.

A problem which prevents these spinel compounds from being applied on an industrial scale is their unstable rechargeability. Even though, the rechargeability has been improved by several groups [1–3], capacity fading on cycling was also observable for those compounds. This was attributed to the fact that a $LiMn_2O_4$ electrode dissolves slowly in the electrolyte solutions [4] and by a Jahn–Teller distortion (cubic Fd3m to tetragonal I4$_1$/amd) occurs caused by a cooperative interaction of the local distortions around Jahn–Teller ions, Mn^{3+} ($t_{2g}^3 - e_g^1$), in octahedral sites [5–7].

Recently, we have developed a simple and cheap route for synthesizing the Li–Mn–O compound system [8]. This involved a direct synthesis by an ionic Na ↔ Li exchange from a sol–gel compound α-$Na_{0.7}MnO_2$. It has been possible to obtain a compound $Li_xMnO_{2+\delta}$ with a high specific capacity and good reversibility [8]. This paper reports the optimum conditions of synthesis and battery performance of $Li_xMnO_{2+\delta}$.

2. Experimental

The average oxidation state, Z_{Mn}, of manganese in the sample was determined by the following procedure. The sample (100 mg) was dissolved in 50 cm^3 of concentrated H_2SO_4, 50 cm^3 of H_2O and in presence of an excess of ferrous(II) ammonium sulphate until complete dissolution. After cooling to 20–25°C the excess of ferrous(II) ammonium sulphate is potentiometrically titrated with potassium permanganate. At the same time a blank is run under identical conditions. Chemical composition of the compounds was made by elemental analysis (inductively coupled plasma–mass spectroscopy: ICP–MS).

The X-ray diffraction (XRD) experiments were performed with a Inel diffractometer using the Cu Kα radiation ($\lambda = 1.540598$ Å). The morphology and the grain size of the samples were performed with a Philips XL 30 scanning electron microscope.

The electrolyte used was 1 mol/l $LiClO_4$, dried under vacuum at 180°C for 15 h, dissolved in a 1:1:1 (volume ratio) mixture of propylene carbonate (PC) ethylene carbonate (EC) and dimethyl carbonate (DMC). The working

* Corresponding author. Tel.: +33-1-49-78-11-43;
fax: +33-1-49-78-13-23.
E-mail address: bach@glvt-cnrs.fr (S. Bach).

Table 1
Chemical formulas and mean oxidation state of manganese, Z_{Mn}, for samples B and C

Sample	Chemical formula	Mean oxidation state of manganese, Z_{Mn}
Sample B	$x(\%)\, Li_{0.7}MnO_{2.27} + y(\%)\,$ lamellar phase $\rightarrow Li_{0.45}MnO_{2.1}$	3.77
Sample C	$Li_{0.52}MnO_{2.1}$	3.70

electrode consisted of a stainless steel grid (7 mm diameter, 0.2 mm thickness) with a geometric area of 1 cm^2 on which the cathode material was pressed (5 t/cm^2). The cathode was made of a mixture of active material (80 wt.%), graphite (7.5 wt.%), acetylene black (7.5 wt.%) and teflon as binder agent (5%). The film is obtained by mixing the oxide powder, carbon and teflon during 10 min for 100 mg of preparation. Electrochemical studies were carried out in
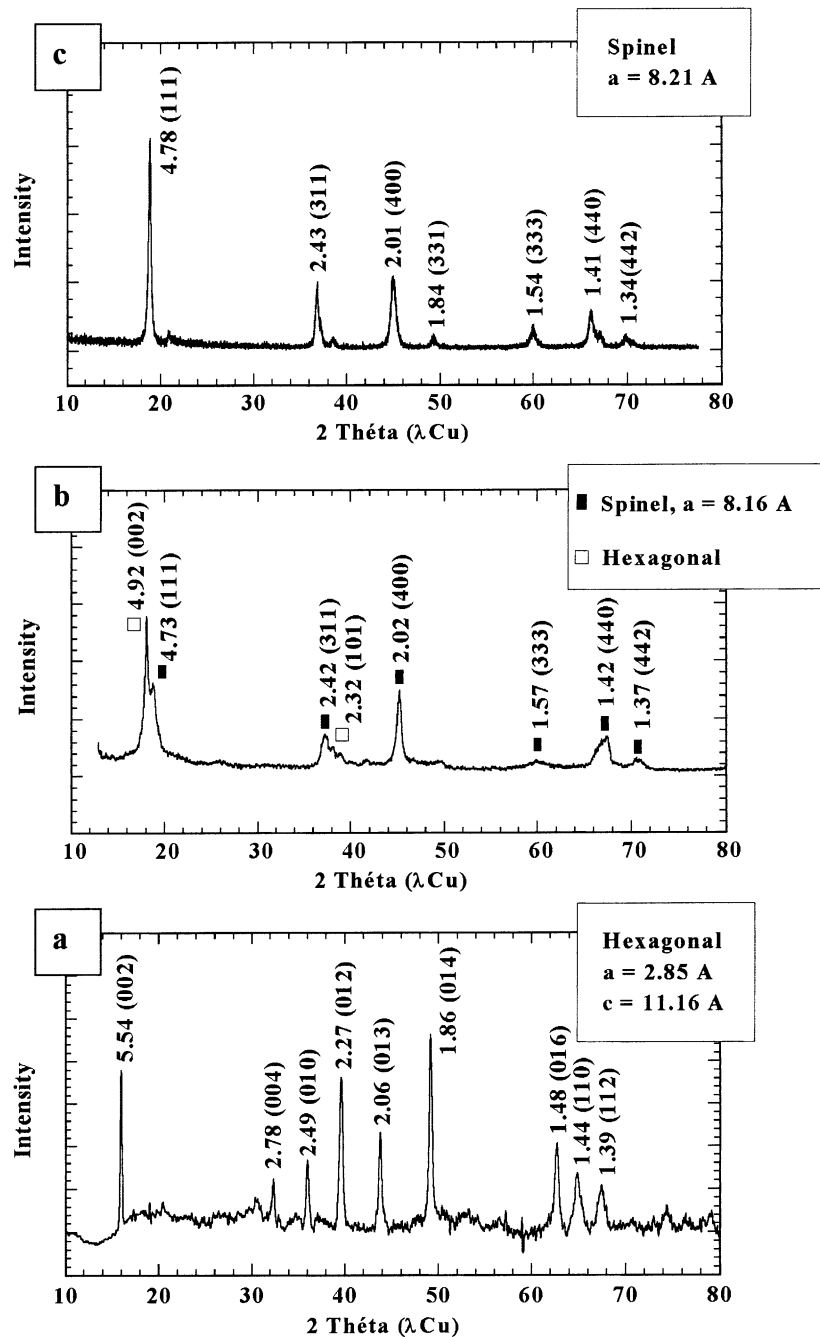

Fig. 1. XRD patterns (Cu Kα) of the sol–gel α-$Na_{0.7}MnO_2$ (a); sample B (b); and sample C (c).

two-electrodes cells (Swagelok® type). This cell was pre-pared inside a dry box by placing a clean lithium metal disk (7 mm diameter), a glass fiber separator soaked with the electrolyte solution, and the cathode pellet into a Teflon container with two stainless steel terminals. Electrochemical measurements were made with a Mac Pile apparatus.

3. Results and discussion

3.1. Synthesis

The α-$Na_{0.7}MnO_2$ (sample A) precursor was synthesized via a sol–gel process. Manganese oxide gels are formed from
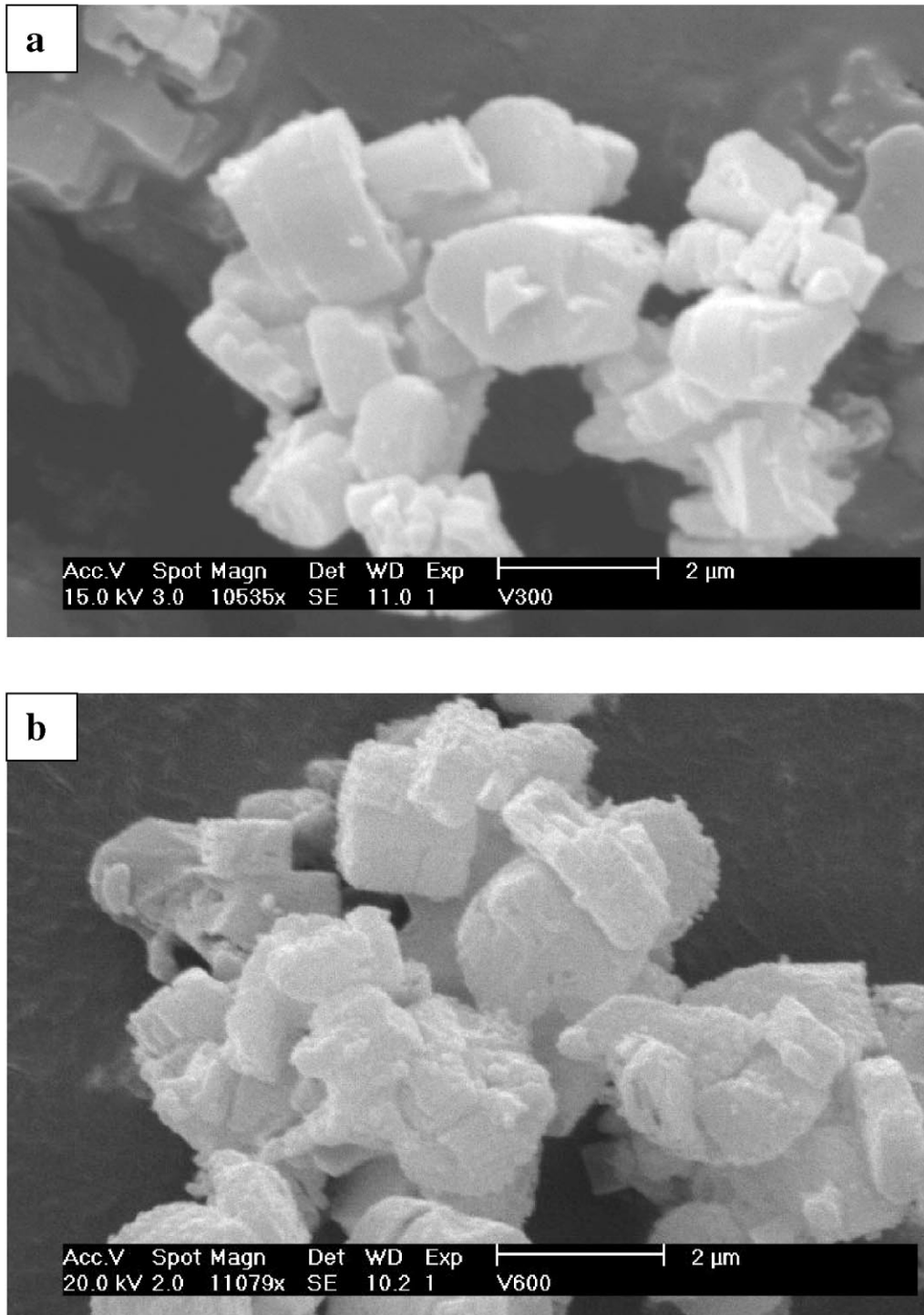

Fig. 2. SEM pictures of sample B (a) and sample C (b).

the reduction of aqueous sodium permanganate solutions $NaMnO_4$ by fumaric acid ($C_4O_4H_4$) [9,10]. Drying and calcination of the gels in which the mean oxidation state of manganese is IV, lead to the formation of the sodium manganese oxide α-$Na_{0.7}MnO_2$ crystalline phase.

The synthesis of $Li_xMnO_{2+\delta}$ was achieved by an ion exchange in aqueous media at 120°C during 48 h to replace the sodium by lithium from the corresponding sodium-containing phase. The resulting powder was then filtered, washed with water and dried at 100°C. The powder has been heated to 300°C at a rate of 10°C/h, maintained at 300°C for 2 weeks (sample B) or at 600°C during 10 h after a thermic treatment at 300°C during 2 weeks (sample C). The chemical formulas and the mean oxidation state determined for each sample are summarized in Table 1.

3.2. Structural studies

The X-ray diffraction pattern of the precursor, α-$Na_{0.7}MnO_2$ is shown in Fig. 1a. It is hexagonal, with the parameters, $a = 2.85$ Å and $c = 11.16$ Å. Its structure consists of layers of edge-sharing MnO_6 octahedra, with Na^+

ions located between these MnO_6 layers. The perpendicular distance between two consecutive layers is 5.54 Å. The XRD pattern of sample B maintained at 300°C for 2 weeks corresponding to curve b in Fig. 1 are characteristic of a mixture consisting of: (i) a spinel phase, as evident from the peaks at 4.73, 2.42, 2.02, 1.57, 1.42 and $d = 1.37$ Å with a unit cell parameter of 8.16 Å and (ii) a lamellar structure isomorph of α-$Na_{0.7}MnO_2$ with a lattice spacing which contracts from 5.54 to 4.92 Å. This mixture was heated at 600°C for 10 h. The XRD patterns of curve c in Fig. 1 reveal that the spinel phase dominates the resulting product with a shift towards higher θ values of the most intensive diffraction line characteristic of the spinel structure ($d = 4.78$ and 2.43 Å) and, a disappearance of the diffraction line at 4.92 Å. The unit cell parameter of the spinel phase at 600°C is $a = 8.21$ Å.

It is well kwown that the unit cell parameter of the cubic spinel $LiMn_2O_4$ is $a = 8.24$ Å [1–3]. The lattice constant decreases with increasing x in the starting material $Li_{1+x}Mn_{2-x}O_4$ or with decreasing the heating temperature as reported before [4,11–13], because the remaining Mn cations become smaller with increasing oxidation state.
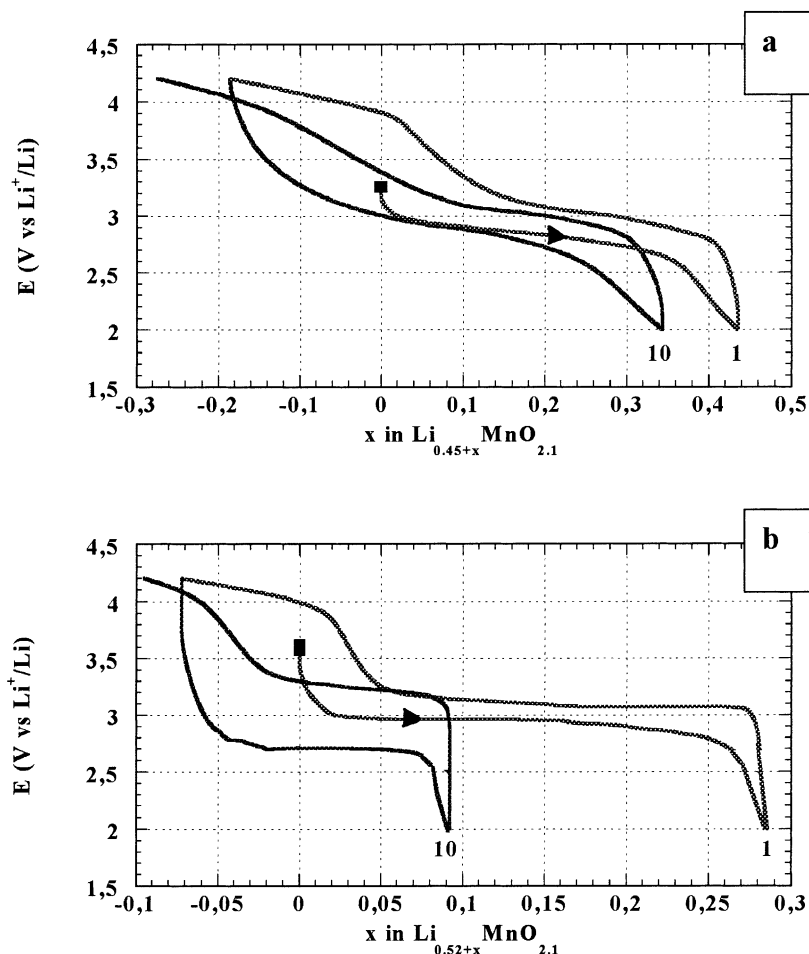

Fig. 3. (a) Chronopotentiometric curves for the first ten reduction oxidation at low current density (C/20 rate) of sample B in a 1 mol/l LiClO$_4$/PC/EC/DMC. (b) Chronopotentiometric curves for the first ten reduction oxidation at low current density (C/20 rate) of sample C in a 1 mol/l LiClO$_4$/PC/EC/DMC.

The calculated lattice parameter of the spinel compound at 600°C ($a = 8.21$ Å) suggests the following formula $Li_{0.99}Mn_{1.9}O_4$ ($Li_{0.52}MnO_{2.1}$) well consistent with the mean oxidation state found ($Z_{Mn} = 3.7$). Calculation of the lattice parameter, a, of the spinel compound in mixture B allows to determine the chemical composition of the cubic phase: $Li_{1.24}Mn_{1.76}O_4$ ($Li_{0.7}MnO_{2.27}$).

The resulting morphology of compounds B and C reveals that the powder grains consist of small ~2 μm crystallites (Fig. 2). The maximum total pore area obtained for the compound at 300°C was measured to 1.75 m²/g, and to 1.63 m²/g for the sample heat-treated at 600°C.

3.3. Electrochemical studies

The electrochemical behavior of these two compounds is shown in Fig. 3. For the compound heat-treated at 300°C (Fig. 3a), which has an initial potential at 3.2 V, an additional 0.44 additional lithium ions are incorporated into the structure during the discharge. This is lower than the Li uptake expected from the initial amount of Mn(IV) in the compound ($Z_{Mn} = 3.84$). The charge process exhibits a well defined single step with 100% efficiency. Moreover, for a cut-off voltage of 4.2 V, the faradaic yield found is higher than that involved on discharge showing that a part of lithium (0.2 Li/mol) originally in the structure can be removed below 4.2 V. An excellent maintenance of capacity is observed during cycling with ~155 mAh/g recovered at the 10th cycle in the voltage 4.2/2 V at C/20 rate.

As far as the compound heat-treated at 600°C is considered, the discharge signal results in a flat voltage plateau near 2.9 V with a faradaic yield of 0.3 F/mol of oxide at C/20 rate. Once again, as previously observed for the "300°C" heat-treated sample, lithium extraction can be achieved from the lattice resulting in the larger discharge capacity on the second cycle. In that case, the capacity decays rapidly after the second cycle to reach only 53% of the initial specific capacity after the 10th cycle.

The present results have illustrated the possibility offered by a new synthesis ways for preparing lithiated manganese oxides with attractive properties. In particular, the interest in the use of a mixture of a spinel and an hexagonal phase with the sample heat-treated at 300°C has been proved.

The impact afforded by the Li ions inside both structures needs deeper structural investigations.

Acknowledgements

References

[1] J.M. Tarascon, W.R. McKinnon, F. Coowar, T.N. Bowmer, G. Amatucci, D. Guyomard, J. Electrochem. Soc. 141 (1994) 1421.
[2] C. Masquelier, M. Tabuchi, K. Ado, R. Kanno, Y. Kobayashi, Y. Maki, O. Nakamura, J.B. Goodenough, J. Solid State Chem. 123 (1996) 255.
[3] T. Tsumura, A. Shimizu, M. Inagaki, Solid State Ionics 90 (1996) 197.
[4] R.J. Gummow, A. de Kock, M.M. Thackeray, Solid State Ionics 69 (1994) 59.
[5] A. Yamada, K. Miura, K. Hinokuma, M. Tanaka, J. Electrochem. Soc. 142 (1995) 2149.
[6] J.B. Goodenough, M.M. Thackeray, W.I.F. David, P.G. Bruce, Rev. Chim. Miner. 21 (1984) 435.
[7] W.I.F. David, M.M. Thackeray, L.A. de Piciotto, J.B. Goodenough, J. Solid State Chem. 67 (1987) 316.
[8] S. Franger, S. Bach, J.P. Pereira-Ramos, N. Baffier, J. Electrochem. Soc. 147 (2000) 3226.
[9] S. Bach, M. Henry, N. Baffier, J. Livage, J. Solid State Chem. 88 (1990) 325.
[10] S. Bach, J.P. Pereira-Ramos, N. Baffier, J. Power Sources 81/82 (1999) 273.
[11] P. Strobel, F. Le Cras, L. Seguin, M. Anne, J.M. Tarascon, J. Solid State Chem. 135 (1998) 132.
[12] M.M. Thackeray, A. de Kock, M.H. Rossouw, D. Liles, J. Electrochem. Soc. 139 (1992) 363.
[13] Y. Xia, M. Yoshio, J. Electrochem. Soc. 144 (1997) 4186.